PAPER

Unraveling the plasma-material interface with real time diagnosis of dynamic boron conditioning in extreme tokamak plasmas

IOP Publishing | International Atomic Energy Agency Nuclear Fusion

Nucl. Fusion **57** (2017) 086050 (7pp) https://doi.org/10.1088/1741-4326/aa7b17

Unraveling the plasma-material interface with real time diagnosis of dynamic boron conditioning in extreme tokamak plasmas

F. Javier Domínguez-Gutiérrez[1], Felipe Bedoya[2], Predrag S. Krstić[1], Jean P. Allain[2], Stephan Irle[3], Charles H. Skinner[4], Robert Kaita[4] and Bruce Koel[5]

[1] Institute for Advanced Computational Science, Stony Brook University, Stony Brook, NY 11749, United States of America
[2] Department of Nuclear, Plasma, and Radiological Engineering, University of Illinois, Urbana, IL 61801, United States of America
[3] Institute of Transformative Bio-Molecules (WPI-ITbM), Nagoya University, Nagoya 464-8602, Japan
[4] Princeton Plasma Physics Laboratory, Princeton, NJ 08543, United States of America
[5] Department of Chemical and Biological Engineering, Princeton University, Princeton, NJ 08544, United States of America

E-mail: predrag.krstic@stonybrook.edu

Received 8 February 2017, revised 2 June 2017
Accepted for publication 22 June 2017
Published 21 July 2017

Abstract

We present a study of the role of boron and oxygen in the chemistry of deuterium retention in boronized ATJ graphite irradiated by the extreme environment of a tokamak deuterium plasma. The experimental results were obtained by the first XPS measurements inside the plasma chamber of the National Spherical Torus Experiment Upgrade, between the plasma exposures. The subtle interplay of boron, carbon, oxygen and deuterium chemistry is explained by reactive molecular dynamics simulations, verified by quantum–classical molecular dynamics and successfully compared to the measured data. The calculations deciphered the roles of oxygen and boron for the deuterium retention and predict deuterium uptake into a boronized carbon surface close in value to that previously predicted for a lithiated and oxidized carbon surface.

Keywords: plasma-surface interactions, boronization, deuterium retention, NSTX-U

(Some figures may appear in colour only in the online journal)

1. Introduction

Plasma-material interface (PMI) science mixes the worlds of plasma and materials, creating in-between a new entity, a dynamical interface that is actively evolving between the two producing one of the most challenging areas of multidisciplinary science. This area has many spatio-temporal fundamental processes and synergies [1–5] driven by both the plasma side of the interface and material transformation on the other. A major goal in PMI science is to extend high-performance plasmas for very long durations and to integrate this performance with plasma-facing components (PFCs) that can withstand high heat and particle fluxes while maintaining structural integrity and minimal retention of fusion fuel [6, 7]. Among the most elusive technical challenges for the advancement of thermonuclear magnetic fusion energy is predictive control of hydrogen recycling in the PFCs as well as management of erosion and defects induced by plasma particle and neutron irradiation [8, 9].

National Spherical Torus Experiment Upgrade (NSTX-U) at the Princeton Plasma Physics Laboratory (PPPL) recently completed, will be the most powerful spherical tokamak experimental fusion facility in the world. It will double the heating power, magnetic field strength (to 1 T) and plasma

current (to 2 MA) of its predecessor, and increase the pulse duration by five times (pulse length 5 s). One of the chasms in deciphering thermonuclear fusion performance has been understanding the causal role that the PMI plays in overall core plasma physics. From the confinement of fuel particles to the impurity emission and retention of particles at the plasma-facing material surfaces, understanding of this complex coupling has remained elusive. This knowledge gap has primarily been driven by the fact that there has been until now no diagnostic that can probe the evolving surface chemistry at the PMI with sufficient accuracy and sensitivity *during and in-between plasma shots*. For the first time an *in situ ex-tempore* technique has been implemented in an extreme tokamak environment and data of the PMI measured with time resolutions of 12–24 h using the Material Analysis Particle Probe (MAPP), newly installed on the NSTX-U chamber [10]. MAPP is capable of performing surface diagnosis between the plasma discharges of samples placed at the wall inside the plasma chamber along the outboard divertor. This is an improvement in time resolution of two orders of magnitude as the traditional approach consisted of examining PFCs *ex situ* and *post-mortem* after an annual campaign consisting of thousands of plasma shots

The first experiments in NSTX-U, performed this year, have explored the effects of boronized carbon (BC) surfaces. Previous experiments with BC PFCs in NSTX [11] and other machines have shown increased plasma confinement time and reduced impurity radiation, in particular oxygen. However, a fundamental understanding of the link between these plasma improvements and the wall surface chemistry remains elusive. This is because the relationship between boronization and actual surface conditions had to be inferred because analysis of PFCs could only be performed at the end of an experimental campaign. In contrast, MAPP has the ability to expose PFC samples to the plasma, and for the first time, analyze them during the course of the run. The time-resolved data obtained with MAPP have enabled comparison with theory to provide unique insight into the detailed chemistry of boronized surfaces.

The key role of oxygen in the uptake of deuterium was deciphered for lithiated carbon PFCs in previous work [6, 7]. In order to establish an understanding of the effects of boronization of PFCs in NSTX-U and fusion wall material surface chemistry in general, we present an experimental and computational studies of the surface chemistry of the deuterium uptake, with particular attention to the mutual chemistry of boron, oxygen, carbon and deuterium. We demonstrate our experimental and computational method in section 2. Our results are presented and discussed in section 3. Finally, we show our concluding remarks in section 4.

2. Methods

2.1. Experiment

The Materials Analysis Particles Probe is a chemical analysis facility designed to characterize samples exposed to tokamak plasmas and conditioning procedures without exposing their surface to atmosphere [12, 13]. MAPP can carry four different samples that are inserted flush with the tiles in the lower divertor of the NSTX-U machine and then be remotely retracted to an analysis chamber for investigation with XPS. In MAPP, XPS is performed with a compact Comstock Hemispherical Analyzer [14] equipped with two Micro Channel Plate (MCP) detectors to collect the photoelectrons signal. The x-ray gun is a water cooled dual anode source (PSP TX400). All the data reported here was collected using a Mg anode ($h\nu = 1253.4$ eV).

MAPP carried two ATJ (fine grain, polycrystalline) graphite, with one TZM (alloy of molybdenum with 0.5% Ti, 0.1% Zr) and one gold sample during the 2015–2016 experimental campaign. Only the data collected with one ATJ sample during one period of boronization (12 d after boron deposition) are reported in this work. The Au sample was used for calibration of the binding energy scale with the $4f_{5/2}$ at 88 eV. The ATJ sample was cleaned with acetone previous to the insertion into MAPP, the samples were then pumped down to 10^{-8} Torr and inserted in the NSTX-U vessel. The inner walls of NSTX-U (including the MAPP's samples) were boronized with a low temperature plasma glow of a mixture of 95% He and 5% deuterated-trimethylboron (d-TMB), details on the boronization procedure can be found in [15]. The boronization was followed by 2 h of Helium glow discharge cleaning (HeGDC) to remove deuterium from the surface of the walls and samples. After this, the samples were retracted to MAPP's analysis chamber for XPS. An XPS data set is formed by a survey scan (1000–0 eV) and three region scans i.e. O 1*s*, C 1*s*, B 1*s*. Following the acquisition of the XPS baselines the samples were reinserted into the tokamak for plasma exposure. The samples were extracted at the end of each day of plasma operations to monitor the chemistry of their surface after the exposures. In a regular day of operations, the NSTX-U executed between 15 and 20 plasma discharges with different plasma configurations, duration and parameters. As a consequence, the ion and particle dose on the samples was different each day.

The procedure was repeated daily during twelve days, after this period the samples were boronized again. The XPS data were analyzed using CASAXPS software to obtain the peaks deconvolution shown in figure 2 and the concentrations shown in figure 1. A detailed literature review added and controlled laboratory experiments were performed to develop a data base with the positions of the peaks in our spectra. The full width at half maximum (FWHM) that constrained the peaks in the regions was obtained with the minimum theoretical resolution of our analyzer i.e. 2 eV [10].

The measurements from MAPP are part of a larger approach of characterization of PFCs that also involves experiments in the laboratory to simulate the conditioning and plasma induced modifications on the surfaces that we observed in the tokamak. The benefits from this approach are twofold i.e. we obtain a clearer description of the processes observed with MAPP in the field and we validate those data and our analysis methodology using equipment with higher energy resolution (~0.5 eV) than that achievable with MAPP's compact analyzer.

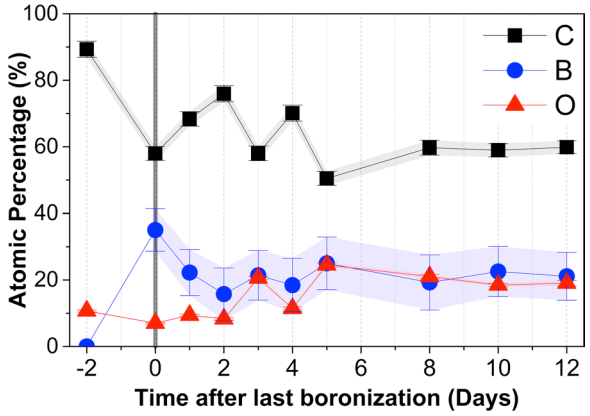

Figure 1. Concentrations of O, B and C measured by XPS in the boronized ATJ graphite sample for increasing plasma exposure. The shaded colored areas are ± one standard deviation about the mean values.

2.2. Computational approach

The qualitative and quantitative chemical evolution of the surface caused by reactive force field (ReaxFF) bond-order potentials [16, 17] is derived from quantum mechanical data, as implemented in the classical-molecular-dynamics (CMD) large scale atomic/molecular massively parallel simulator (LAMMPS) code [18]. Besides, the ReaxFF approach describes atomic charge dynamics due to the change of atomic coordinates during the deuterium impact cascade [16, 17]. This advantage of ReaxFF is based on the electrochemical electronegativity equalization method, a semi-empirical method which applies a set of pre-calibrated, material and coordinate dependent parameters to recalculate charges at each MD step [17].

We constructed amorphous samples of 400 atoms for various predefined, energy-optimized surface configurations of BC, CO and BCO that were thermalized at 300 K, with periodicity established in the direction parallel to the surface and with deuterium atoms impinging orthogonal to the prepared surface. We use the ReaxFF potentials reported in [17] to perform MD simulations.

The boronized and oxidized carbon surface was prepared as an amorphous virgin B–C–O cell with about 400 atoms. This cell has a predefined initial atomic distribution of 20% O, 20% of B, and 60% of C approximately mimicking the experimental data shown in figure 1. The cell is energy optimized by the consecutive process of heating and annealing and finally thermalized to 300 K using Langevin thermostat. The resulting cell has lateral dimensions of 1.75 nm in z-direction and about 1.5 nm in x and y directions. This maximal penetration of a D atoms of 5 eV impact energy, tested with 3000 impacts, is about 0.75 nm. Therefore the computation cell is large enough to avoid artificial reflections of deuterium atoms by the cell bottom. Consequently, our identification of the surface chemistry, including determination of the concentrations of various atomic constituents of the target surface as response to the deuterium impacts in z-direction, are performed only in the upper half of the cell (table 1). 2D periodic boundary conditions (in x and y directions) are applied during all steps of our simulations.

Table 1. Percentage of C, B, O, and deuterium accumulated in the upper half of the four target cells. The C, B, O percentages without D are normalized to 100% for comparison to XPS data.

Deuterium	Carbon	Boron	Oxygen
0	55.07	23.91	21.02
12.50	56.62	22.79	20.59
23.91	55.80	23.19	21.01
38.24	56.62	22.79	20.59

The preparation of the deuterated B–C–O surface by D-accumulation was done by cumulative bombardment by D atoms at 5 eV. The separation time between successive D impact was 50 ps, of which 20 ps is for the thermostat-independent cascade evolution, 20 ps is the target thermalization to 300 K and 10 ps is relaxation time. The cumulative process created surfaces with 12.5%, 24% and the maximum 38% of D, calculated from $D_{acc} = N_D/(N_C + N_B + N_O)$. The data showing the concentrations of D, C, B and O for four target surfaces used in this work are shown in table 1.

Upon the surfaces preparation, we have bombarded each sample with 3000 independent 5 eV D impacts perpendicularly to the surface in order to reach statistical accuracy in the data. Although each of these D atoms impacted the same surface, thus probing the surface with just one additional D atom, the locations of the impacts were randomly distributed over the surface. This procedure reduced the maximal standard error of the obtained chemistry of a retained D atoms, as well as of the induced chemistry in the surface mixture of B, C, and O to less than the size of symbols at figures 3 and 4.

We have verified our results for the D retention chemistry with the quantum–CMD calculations using the self-consistent-charge tight-binding density functional method (SCC-DFTB) [19, 20]. Though there is a qualitative difference of the REAXF and SCC-DFTB results ranging within 20% no difference in the phenomenology of the results was found. The comparison was published in [21].

3. Results and discussion

We compare atomistic simulations, as explained in section 2.2, to experimental x-ray photoelectron spectroscopy (XPS) measurements, as described in section 2.1. We report XPS measurements at the end of each day after exposure of the MAPP sample to deuterium plasmas. Thus, these data represent the cumulative effect of plasma exposure and between-shot He-GDC. They discriminate, however, against the outgassing between the run days.

The measured evolution of the surface elemental concentrations are shown in figure 1. This was obtained by quantitative analysis using the XPS spectra. Details on this procedure can be found in [11].

Prior to the boronization, the oxygen surface concentration on the ATJ graphite MAPP sample was about 12% (atomic percent, excluding hydrogen since XPS is unable to measure the D concentration directly). Upon boronization, the oxygen concentration decreased to 6% and the other surface constituents were 35% of B and 59% of carbon. Following 5 d of plasma

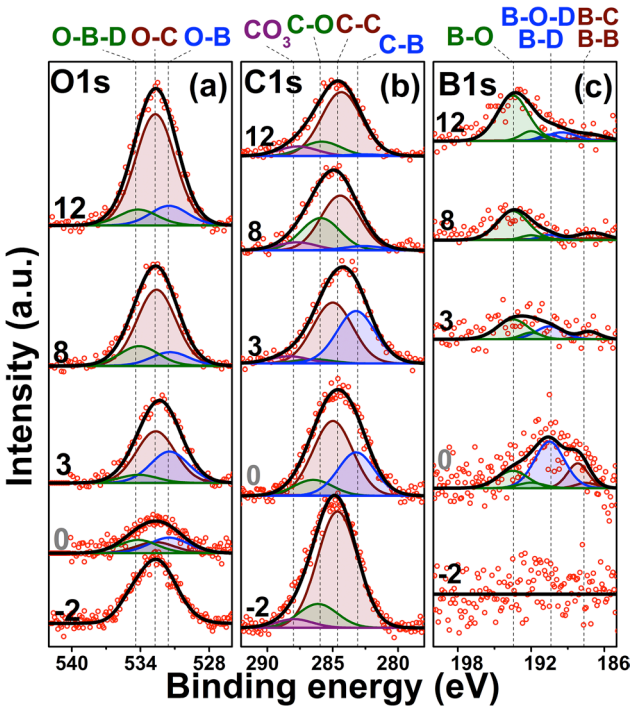

Figure 2. (*a*) O 1*s*, (*b*) C 1*s*, and (*c*) B 1*s* XPS spectra from boronized ATJ graphite for various days of deuterium plasma exposure. Day '0' is the day of boronization and the spectra shown were obtained immediately after boronization.

operations, the oxygen concentration increased to about 20%, while the boron and carbon reached about 20% and 60%, respectively. The oxidation of boron coatings on graphite has been previously observed in laboratory experiments where samples were exposed to oxygen ions [22]. A 5% to 35% increase of oxygen content upon deuterium bombardment in lithiated carbon surfaces of NSTX has been also observed [6, 7]

Figure 2 shows the O 1*s*, C 1*s*, and B 1*s* core-level XPS signals after daily exposures to deuterium plasma corresponding to the time intervals shown in figure 1. Decomposition into the constituent XPS peaks is based on [10], guided also by our atomistic simulations. The chemical changes are observed as simultaneous shifts and intensity changes in the O 1*s*, B 1*s* and C 1*s* spectra. Thus, formation of O–B bonds is assigned to peaks at 531.5 eV and O–B–D to peaks at 534.5 eV in the O 1*s* signal, while the B 1*s* peak at 190.5 eV is assigned to B–O–D and B–D species. The C 1*s* peak at 283 eV is assigned to C–B bonding and the B 1*s* peak at 187.5 eV peak to B–C and B–B bonding. These assignments vary slightly from Ghezzi *et al* [23] due to experimental setup differences.

We perform CMD simulations of deuterium irradiation on boronized, deuterated, and oxidized carbon surfaces, following the approach and surface configurations described in section 2.2. For each of the O, C, and B atoms we calculate distances to the nearest neighbors to determine its proper coordination and thus, its strongest favorable bonds [8] as functions of the D concentration. The bond length thresholds are estimated by covalent lengths of the constituent atoms. Since these were found to deviate as much as 20% in SCC-DFTB, and as much as 30% in REAXFF calculations, visual inspection was done for each bond, and in some cases this was

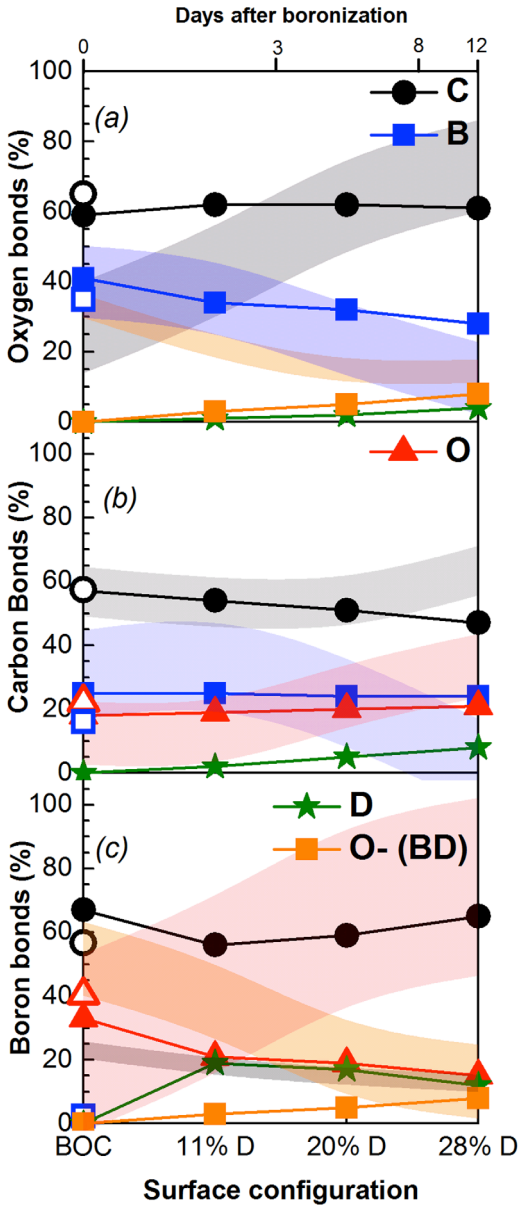

Figure 3. Percentage of bonds of (*a*) O, (*b*) C, and (*c*) B to other constituents in the BCOD surface as a function of D concentration in the upper 7.5 Å of the computed sample. The surface was irradiated randomly with over 3000 deuterium atoms at 5 eV for each of accumulated D concentrations, leading to a small statistical error in figure, smaller than a symbol size. The shaded colored areas, bands, are ± one standard deviation about the mean values measured by XPS of the corresponding bonding (color matched to the calculated values, grey is C, pink is O, light-blue is B, yellow is B–O–D), averaged over the 4 d of plasma exposure in figure 2. CO_3 was counted as triple match, and joined to the C–O band. Additional simulations and measurement analysis will be needed in the future to decipher the time-dependent D accumulation evidence in the MAPP data.at the expense of boron with carbon. This is also indicated by the increasing behavior of C–O bonding from 27% to 76% in the O 1*s* scans (which is hidden in flat bands) that also indicates the dominance of oxygen atoms at the surface.

supplemented by the electron density analysis. Figure 3 shows the favorable bonding for each of the atoms in %, normalized to the total number of atom bonds of the particular type. Thus, for oxygen bonds, the number of O–B, O–C and O–D bonds

are normalized to the total number of oxygen bonds in the top 0.75 nm of the considered computational cell.

The amounts of O–B, O–C, and O–B–D bonding in figure 3(*a*) are consistent with those in the top three blocks of figure 2(*a*): O–C slightly increases and O–B decreases, respectively, while O–B–D slightly increases with plasma exposure. However, as mentioned in the caption of figure 3, the goal of this work is not to follow the time dependent effects of the D accumulation, since these effects are not well defined with this experiment. Note that the BCO point at the horizontal axis of figure 3 corresponds to zero accumulation of D. The bands in figure 3 were obtained averaging the concentrations of two consecutive days of the data shown in figure 2. The values at the BCO abscise were obtained from the data labeled with '0' at figure 2. The values from the XPS spectra indicate a non-trivial concentration of D in the BCO system likely due to the plasma-enhanced deposition of boron films with D atoms from the gas phase during molecular dissociation during deposition. This would result in a higher value from simulations of the O-(BD) and lower B–O complex. The simulated C–C, C–O, C–B and C–D curves in figure 3(*b*) are consistent with the colored bands emerging from measurements in figure 2(*b*). We note that the simulated values in figure 3(*b*) were rescaled, after the C–C concentration at 11% and 20% D was fitted to the middle of the measured C–C peak intensity. This was done because the depth probed by XPS (a few nm) is much deeper than the surface layers involved in the calculation (0.75 nm). There are discrepancies however found in the B–C and B–O interactions both in the B 1*s* time-dependent spectra. In particular, there is a non-trivial variation of the measured B–C interaction in the C 1*s* scan region decreasing from ~31%–42% down to only 2–4%.

The bands of strong B–O and B–C peaks in figure 3(*c*), do not fit well with calculated curves. On the other hand, the dominance of B–D and B–O–D XPS peaks was established immediately after boronization by $B(CD_3)_3$ (day '0' in figure 2). This brought a significant amount of D into the surface, which then decreases in time in figure 2(*c*), due to the He-GDC and outgassing. This trend in D content as well as of the B–O–D is well reflected by the relevant calculated curves in figure 3(*c*).

Consistent with the 'discrepancies' of flipped C and O behavior between experiment and simulation in B 1*s* we find that the 'time' of exposure of D irradiation is driving oxygen to the surface and increasing the effective oxygen content dynamically and thus dominating bonding between oxygen and boron atoms

Since simulations in figure 3 keep the oxygen concentrations static, a number of runs were completed that increased oxygen at the surface to 40%. These results are indicated in figure 3 as 'open symbols'. The results are consistent with our conjecture that there is a mechanism responsible for driving oxygen to the surface similar to those found for lithiated graphite [6, 7]. This finding is particularly critical for the large discrepancy in functional behavior of the B–O and B-(OD) XPS data with exposure time (e.g. days after boronization) in figure 3(*c*).

The high degree of qualitative and quantitative agreement between the theoretically anticipated and measured chemistry in the complex BCOD surface allows us to analyze the

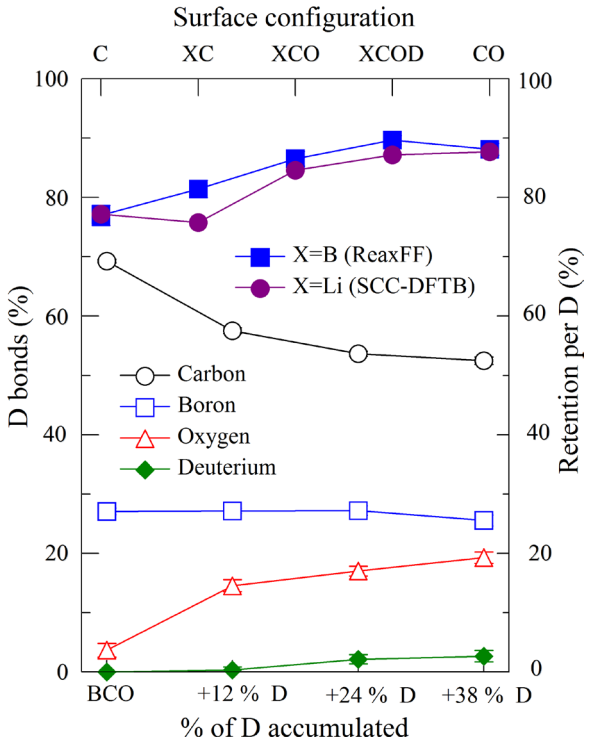

Figure 4. Percentage of D bonds with constituents of the BCOD surface as function of the deuterium accumulated concentration (left axis). Retention per impact of D on BCOD and LiCOD (right axis).

deuterium retention chemistry and yield per D, shown in figure 4. The initially negligible role of oxygen in bonding D in the BCO (<5% of D is bonded to O) is changed significantly with D uptake, reaching almost 20% of D, in strong contrast to the role of oxygen in the D retention of LiCO surfaces [8].

Boron in general is more reactive than carbon because of the so-called octet rule, i.e. a coordination number of four is preferred for B atoms even so it only has three valence electrons, and in our simulations we sometimes even find coordination numbers of five and six. Also electron withdrawing ligands on B such as O further increase D uptake on B. Thus, the role of B in the retention of D does not change with increasing D accumulation as can be seen in figure 4. However, the role of carbon in D retention decreases with D accumulation, since C is less flexible in its coordination number than B. Considering the unchanged role of B in D binding, more of the impacting D is available to bond to O. Besides, the accumulated D bonds to the O binding partner B as in figures 3(*a*) and (*c*), creating BCD and destroying boron bonds to O, thereby making room for O–D. This situation contrasts to the case of LiCO where Li does not play a significant role in D bonding. It is rather oxygen that plays the major role, as it is retained in high concentration in the surface due to the long range interactions of Li and O [6].

The atomic content of D in the surface was not directly measured by XPS, but can be estimated from the XPS peak intensities corresponding to B-(OD) and O–B–D bonding in figure 2. The agreement of our simulations with the trends observed in the XPS spectra for the various BCO components indicates that the D concentration in the surface increases with the cumulative plasma exposures after boronization.

According to the results shown in figure 4, about 80% of D is retained in the BC surface. This is about 5% more than the % D retained in the LiC surface previously reported in [6, 7, 24]. However, when the 20% of carbon atomic concentration is replaced by oxygen, D retention in BCO and LiCO [8] surfaces is 86.5% and 84.5%, respectively. With accumulated D, the D retention reaches 89.6% for BCOD and 86% for LiCOD. The similarity of the retention curves for various matrices containing Li and B, in spite of different chemistry, is unexpected, having in mind the different chemistry of D-retention in Li and B matrices and the reduction in the divertor D-alpha emission with lithium consistent with a drop in recycling coefficient from $R \sim 0.98$ to $R \sim 0.9$ [25]. The B matrices hold a few percent more D than the Li matrices, a consequence of the B atoms having strong chemical reactivity and variability in their coordination number.

4. Concluding remarks

The implications of this work are far-reaching given for the first time our ability to observe '*in situ*' the complex surface chemistry and physics induced by exposure of device walls to the extreme environment in tokamak plasma that combines three states of matter. The results also reflect new insights into the irradiation-driven mechanisms that drive hydrogen retention at evolving surfaces and dictate the coupling of plasma and the wall, both critical fundamental *and* practical aspects of fusion energy. One significant contribution of this work is that for the first time the evolving, reconstituted surface exposed to a tokamak plasma in the first 4–8 nm is dynamically measured and the findings elucidate the critical role played by oxygen in the condensed matter state. This aspect of plasma-facing surfaces and the critical role surface chemistry plays on hydrogen retention is beginning to bring a new understanding of how surface impurities and their balanced interaction with plasma chemistry could influence bulk plasma behavior.

Furthermore, this work also involves the use of advanced computational atomistic simulations of the chemistry inside the irradiated surface, validated with *in situ ex-tempore* measurements of low-energy deuterium irradiation of boron-treated graphite samples introduced in the NSTX-U divertor region. The understanding of the computed chemistry dynamics in the studied quaternary material surface, containing C, B, O and D, allowed us to predict with confidence the deuterium uptake in the surface, for various D concentrations, as well as the role of various surface components in this uptake. Combining these atomistic simulations with the dynamic measurements of chemical states by MAPP is the greatest strength of this work as both cover different spatial and temporal scales that when combined elucidate key D retention mechanisms.

Acknowledgment

This material is based upon work supported by the National Council for Science and Technology of Mexico (CONACyT) through the postdoctoral fellowship CVU 267898 (FJDG), by the USDOE FES Grant No. DE-SC0013752 through RF of SUNY (PSK), by the USDOE BES/FES Grant No. DE-SC0010717 (JPA and FB), and by DOE FES Grant No. DE-SC0012890 (BEK). Simulations were obtained using the LI-red cluster at the IACS-SBU, and by the NCCS supercomputing facility in ORNL.

ORCID

F. Javier Domínguez-Gutiérrez https://orcid.org/0000-0002-1429-0083
Predrag S. Krstić https://orcid.org/0000-0002-2966-7082
Jean P. Allain https://orcid.org/0000-0003-1348-262X

References

[1] Leonard A.W. *et al* 1997 Distributed divertor radiation through convection in DIII-D *Phys. Rev. Lett.* **78** 4769
[2] Abromeit C. 1994 Aspects of simulation of neutron damage by ion irradiation *J. Nucl. Mater.* **216** 78
[3] Kallenbach A. *et al* 2011 Overview of ASDEX upgrade results *Nucl. Fusion* **51** 094012
[4] Soukhanovskii V.A. *et al* 2009 Divertor heat flux mitigation in high-performance H-mode discharges in the National Spherical Torus Experiment *Nucl. Fusion* **49** 095025
[5] Federici G. *et al* 2001 Plasma-material interactions in current tokamaks and their implications for the next step fusion reactors *Nucl. Fusion* **41** 1967
[6] Krstic P.S. *et al* 2013 Deuterium uptake in magnetic-fusion devices with lithium-conditioned carbon walls *Phys. Rev. Lett.* **110** 105001
[7] Taylor C.N., Heim B. and Allain J.P. 2011 Chemical response of lithiated graphite with deuterium irradiation *J. Appl. Phys.* **109** 053306
[8] Zinkle S.J. 2005 Fusion materials science: overview of challenges and recent progress *Phys. Plasmas* **12** 058101
[9] Skinner C.H. *et al* 2013 Plasma facing surface composition during NSTX Li experiments *J. Nucl. Mater.* **438** S647
[10] Bedoya F. *et al* 2016 Unraveling Wall conditioning effects on plasma facing components in NSTX-U with the materials analysis particle probe *Rev. Sci. Instrum.* **87** 11D403
[11] Skinner C.H. *et al* 2002 Effect of boronization on ohmic plasma in NSTX *Nucl. Fusion* **42** 329
[12] Taylor C.N. *et al* 2012 Materials analysis and particle probe: A compact diagnostic system for *in situ* analysis of plasma-facing components (invited) *Rev. Sci. Instrum.* **83** 10D703
[13] Lucia M. *et al* 2014 Development progress of the materials analysis and particle probe *Rev. Sci. Instrum.* **85** 11D835
[14] Comstock Electrostatic energy analyzer manual, Comstock Incorporated, Oak Ridge, TN, USA
[15] Skinner C.H., Allain J.P., Bedoya F., Blanchard W., Cai D., Koel B. and Scotti F. 2017 Advances in boronization on NSTX- upgrade *Nucl. Mater. Energy* (https://doi.org/10.1016/j.nme.2016.11.024)
[16] van Duin A.C.T., Dasgupta S., Lorant F. and Goddard W.A. 2001 ReaxFF: a reactive force field for hydrocarbons *J. Phys. Chem.* A **105** 9396
[17] Weismiller M.R., van Duin A.C.T., Lee J. and Yetter R.A. 2010 ReaxFF reactive force field development and applications for molecular dynamics simulations of ammonia borane dehydrogenation and combustion *J. Phys. Chem.* A **114** 5485

[18] Plimpton S. 1995 Fast parallel algorithms for short-range molecular dynamics *J. Comput. Phys.* **117** 1–19
[19] Elstner M. *et al* 1998 Self-consistent-charge density-functional tight-binding method for simulations of complex materials properties *Phys. Rev.* B **58** 7260
[20] Zheng G. *et al* 2007 Implementation and benchmark tests of the DFTB method and its application in the ONIOM method *Int. J. Quantum Chem.* **109** 1841
[21] Dominguez-Gutierrez F.J. *et al* 2017 Studies of lithiumization and boronization of ATJ graphite PFCs in NSTX-U *Nucl. Mater. Energy* (https://doi.org/10.1016/j.nme.2016.12.028)
[22] Alimov W.K., Zalavutdinov R.K. and Scherzer B.M.U. 1994 Oxygen retention in D-ion-irradiated B_4C and boron-doped graphite *J. Nucl. Mater.* **212** 1461
[23] Ghezzi F. *et al* 2015 XPS, SIMS and FTIR-ATR characterization of boronized graphite from the thermonuclear plasma device RFX-mod *Appl. Surf. Sci.* **354** 408
[24] Krstic P.S. *et al* 2012 Dynamics of deuterium retention and sputtering of Li–C–O *Fusion Eng. Des.* **87** 1732
[25] Canik J.M. *et al* 2011 Measurements and 2D modeling of recycling and edge transport in discharges with lithium-coated PFCs in NSTX *J. Nucl. Mater.* **415** S409